

Nanoscale localization of poly(vinylidene fluoride) in the lamellae of thin films of symmetric polystyrene–poly(methyl methacrylate) diblock copolymers

Seong Il Yoo^a, Sang-Hyun Yun^a, Jeong Min Choi^a, Byeong-Hyeok Sohn^{b,*}, Wang-Cheol Zin^a, Jin Chul Jung^a, Kwang Hee Lee^c, Seong Mu Jo^d, Junhan Cho^e, Cheolmin Park^f

^aDepartment of Materials Science and Engineering, Pohang University of Science and Technology, Pohang 790-784, South Korea

^bDepartment of Chemistry, NANO Systems Institute, Seoul National University, San 56-1 Sillim-dong Gwanak-gu, Seoul 151-747, South Korea

^cDepartment of Polymer Science and Engineering, Inha University, Incheon 402-751, South Korea

^dPolymer Hybrid Research Center, Korea Institute of Science and Technology, Seoul 130-650, South Korea

^eDepartment of Polymer Science and Engineering, Dankook University, Seoul 140-714, South Korea

^fDepartment of Metallurgical System Engineering, Yonsei University, Seoul 120-749, South Korea

Received 14 September 2004; received in revised form 21 February 2005; accepted 14 March 2005

Available online 7 April 2005

Abstract

We employed thin film blends of diblock copolymers with functional homopolymers as a simple strategy to incorporate organic functional materials into nanodomains of diblock copolymers without serious synthesis. A blend pair of polystyrene–poly(methyl methacrylate) (PS–PMMA) diblock copolymers and poly(vinylidene fluoride) (PVDF) was selected as a model demonstration because PVDF is a well-known ferroelectric polymer and completely miscible with amorphous PMMA. Thin films of symmetric PS–PMMA copolymers provided the nanometer-sized PMMA lamellae, macroscopically parallel to the substrate, in which PVDF chains were dissolved. Thus, amorphous PVDF chains were effectively confined in the PMMA lamellae of thin film blends. The location of PVDF chains in the PMMA lamellae was investigated by the dependence of the lamellar period on the volume fraction of PVDF, from which we found that PVDF chains were localized in the middle of the PMMA lamellae. After the crystallization of PVDF, however, some of PVDF migrated to the surface of the film and formed small crystallites.

© 2005 Elsevier Ltd. All rights reserved.

Keywords: Diblock copolymers; Thin films; Blends

1. Introduction

Block copolymers self-assemble into periodic structures in the tens of nanometer length scale. The size and morphology of self-assembled domains can be easily controlled by adjusting the molecular weight and composition of the copolymers [1]. In addition, the functionality of the nanodomains can be tailored by selection of the chemical type of each block [2,3]. To utilize this self-assembled nanostructure of block copolymers in potential applications for nanoscale devices, block copolymers

should be fabricated in the shape of thin films on the solid substrate [2–6].

By periodic nanodomains of diblock copolymers in thin films, for example, nanoscale lithographic masks for etching processes and templates for deposition of electronic components in the nanometer range were produced [2–6]. Also, self-assembled nanodomains of diblock copolymers in thin films were utilized to generate periodic functional nanostructures by selective incorporation of nanoparticles of metals, semiconductors, or oxides into one of the blocks [7–14]. For instance, thin films of symmetric diblock copolymers were employed to generate self-assembled multilayers of periodic repeats of pure polymeric layers and nanoparticle-functionalized layers, which are potentially useful for electronic and photonic applications [13]. Moreover, in thin films of symmetric diblock copolymers,

* Corresponding author. Tel.: +82 2 883 2154; fax: +82 2 889 1568.
E-mail address: bhsohn@snu.ac.kr (B.H. Sohn).

macroscopically oriented multilayers parallel to the substrate in long-range order can be generated due to the preferential interaction of one of the blocks to the substrate or the air interface [15–19].

To make nanodomains of block copolymers electrically or optically active, organic functional materials, instead of inorganic nanoparticles, can be incorporated or synthesized selectively to one of the blocks [2,3]. For example, it was possible to incorporate conducting polymers in nanometer-sized domains by their selective synthesis within the periodic nanostructure of diblock copolymers [20].

In this study, we employed the blending method of diblock copolymers with functional homopolymers as a simple strategy to demonstrate incorporation of organic functional materials into nanodomains of diblock copolymers in thin films without intensive synthesis. A blend pair of polystyrene–poly(methyl methacrylate) (PS–PMMA) diblock copolymers and poly(vinylidene fluoride) (PVDF) [21–23] was selected as a model demonstration because PVDF is a well-known ferroelectric polymer and completely miscible with amorphous PMMA below the lower critical solution temperature of ca. 350 °C [23]. Thin films of symmetric PS–PMMA copolymers were employed not only because the shape of thin films is necessary for practical applications, but also because their multilayered structure with a film thickness quantized in terms of the lamellar period enabled us to quantify the dependence of the lamellar period on the volume fraction of PVDF simply by thickness measurements [24,25]. From this dependence, homogeneous distribution or local segregation of PVDF in the PMMA domain can be evaluated. We found that PVDF chains were confined in the PMMA lamellae of the thin film blend but were segregated in the middle of PMMA lamellae. After crystallization of PVDF, however, some of PVDF migrated to the surface of the film and formed small crystallites.

2. Experimental section

Symmetric polystyrene–poly(methyl methacrylate) (PS–PMMA) diblock copolymers were purchased from Polymer Source Inc. The number average molecular weights of PS and PMMA were 25,000 g/mol and 26,000 g/mol, respectively. The polydispersity index was 1.09 and the styrene volume fraction was 0.52. Relatively low molecular weight poly(vinylidene fluoride) (PVDF) with the weight-average molecular weight of 6,600 g/mol were used. The crystallization and melting temperatures of the low molecular weight PVDF measured by a differential scanning calorimeter (scanning rate = 5 °C/min) were 133 and 169 °C, respectively. The values were lower than those of typical PVDF.

Silicon wafers (ca. $1.5 \times 1.5 \text{ cm}^2$) were cleaned in a piranha solution (70/30 v/v of concentrated H_2SO_4 and 30%

H_2O_2) at 90 °C for 20 min, and thoroughly rinsed with deionized water several times, and then blown dry with nitrogen.

PS–PMMA copolymers and PVDF were dissolved in dimethylacetamide, DMAc, to yield 2.0–5.0 wt% solutions with various volume fractions of PVDF homopolymers in entire samples, ranging from 0 to 0.30. Thin film blends of PS–PMMA and PVDF were spin-coated onto clean silicon wafers from DMAc solutions. Film thicknesses were adjusted by spinning speeds (1500–5000 rpm) and solution concentrations (2.0–5.0 wt%). The spin-coated films were annealed at 180 °C, above the glass transition temperatures of PS and PMMA and the melting temperature of PVDF, but below the lower critical solution temperature of the blend of PMMA and PVDF, for 24 h in a vacuum oven. After annealing, the films were quenched down by dipping into liquid nitrogen to avoid the crystallization of PVDF. Then, the films were annealed again at 133 °C, the crystallization temperature of PVDF, for 5 h to induce the crystallization of PVDF.

Surface topography of thin films was imaged using an AFM (AutoProbe CP Research, Park Scientific Instruments) in contact mode. After scraping away some of the film from the substrate with a razor blade, the film thickness was measured from several different areas to obtain an average value.

Transmission electron microscopy (TEM) was performed on a JEOL 1200EX operating at 120 kV. TEM samples were prepared as described in the literature [13]. From the thin film embedded in epoxy with carbon coating on both sides of the film after removing the substrate, thin sections (ca. 70 nm thick) were obtained using a Reichert Ultra Microtome with a diamond knife. Samples were exposed to RuO_4 (0.5% aqueous solution) for about 10 min to stain the PS block selectively.

To investigate the crystalline form of PVDF, Fourier-transformed infrared (FTIR) spectra on thin film blends of PS–PMMA and PVDF after the crystallization of PVDF were recorded on a Mattson Infinity Gold spectrophotometer in attenuated total reflection (ATR) mode. A thin film of the blend was directly coated on a zinc selenide crystal ($25 \times 10 \times 3 \text{ mm}^3$).

3. Results and discussion

Since the PS block has a lower surface energy and the PMMA block has a preferential interaction to polar native oxide layers of silicon wafers, multilayered lamellae of symmetric PS–PMMA diblock copolymers parallel to the substrate are induced on silicon wafers in an asymmetric wetting configuration [15,16], i.e. the PMMA block at the substrate interface and the PS block at the air interface, with a quantized film thickness of $(n + 1/2)L_0$, where n is a positive integer and L_0 is the lamellar period. When the initial film thickness is not commensurate with the

constraint of $(n + 1/2)L_0$, terraces (holes or islands) form on the free surface of the film with the step height of L_0 [15–19]. Holes or islands form only when the lamellae are ordered in the direction parallel to the substrate. Therefore, the lamellar period of PS–PMMA diblock copolymers and its change after mixing with PVDF can be evaluated simply by measuring the film thickness and the terrace height with AFM [14,24,25].

A typical AFM image of the surface of pure PS–PMMA thin films before mixing with PVDF is shown in Fig. 1. The initial film thickness before annealing was 70.6 nm in average ($2.8L_0$). This value was between 2.5 and $3.0L_0$ so that island formation was expected on the top of a $2.5L_0$ -quantized film after annealing. Thus, the film had a quantized thickness of $2.5L_0$ with islands in a step height of L_0 , as shown in Fig. 1.

A cross-sectional TEM image of a PS–PMMA thin film shown in Fig. 2 clearly shows the multilayered structure in the film. PS lamellae appeared as darker regions due to RuO_4 staining. Since this TEM image was obtained from the area under the island of Fig. 1, the multilayered structure had $3.5L_0$ (the quantized thickness of $2.5L_0$ + the step height of L_0), consisting of 3.5 PS lamellae and 3.5 PMMA lamellae. It should be noted that typical lateral dimensions of islands were a few micrometers, which were far larger than the size of the TEM image in Fig. 2. Apparently PS lamellae were thicker than PMMA lamellae due to staining and additional thinning of the PMMA block by electron irradiation in TEM, which made it difficult to quantify changes of the lamellar period in thin film blends by TEM analysis.

From the film thickness and the island height, the

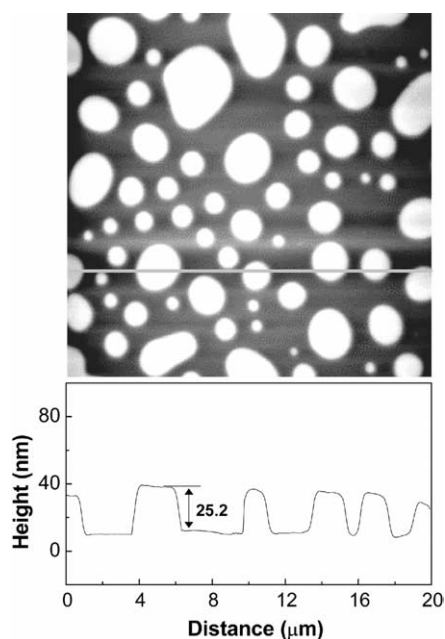


Fig. 1. AFM image of the surface of a PS–PMMA thin film with islands in a step height of L_0 . Islands in the film appear as bright areas. Along the line in the image, height profile is given below the image.

lamellar period (L_0) of pure PS–PMMA thin films before blending with PVDF was evaluated as 25.2 nm (± 0.9 nm). This value was somewhat smaller than that (29.8 nm) obtained from the small-angle X-ray scattering (SAXS) measurement on the bulk PS–PMMA. Probably this discrepancy would be associated with the contact-mode measurement of AFM as well as the sample geometry, although exact reasons were not clear yet. However, all the lamellar periods in thin film blends were also evaluated from AFM measurements and compared with one another so that this discrepancy would not be crucial in this study.

In a similar way, we evaluated variations of the lamellar period (L) of thin film blends of PS–PMMA diblock copolymers and PVDF from a quantized film thickness of $(n + 1/2)L$ and a terrace height of L . Fig. 3 shows a typical surface image of thin film blends of PS–PMMA and PVDF when the volume fraction of PVDF was 0.13. The initial film thickness of this thin film blend before annealing was 94.5 nm in average ($3.1L$), which was between 3.0 and $3.5L$ so that hole formation was expected on the surface of the $3.5L$ -quantized film after annealing. It should be noted that L is the lamellar period in the case of thin film blends. Thus, holes appeared as dark areas with an average depth of 30.5 nm (± 1.0 nm) in Fig. 3. From these AFM measurements, variations of the lamellar period (L) as a function of the volume fraction of PVDF (ϕ_{PVDF}) are shown in Fig. 4. When volume fractions of PVDF in the blends were higher than 0.3, films were not spin-coated on the substrate from DMAc solutions of the blends so that the case of high PVDF contents was not considered in this study.

In all thin film blends of PS–PMMA and PVDF with ϕ_{PVDF} lower than 0.3, hole or island formation was observed on the film surface. This result implied that multilayers of lamellae parallel to the substrate were induced in thin film blends of PS–PMMA and PVDF without macro-phase separations and morphological transitions. Since PVDF chains are miscible only with the PMMA block of PS–PMMA diblock copolymers, they should be mixed in the PMMA lamellae. Thus, PVDF chains were effectively confined in the PMMA lamellae of thin film blends. Also, the PVDF chains mixed in the PMMA lamellae resulted in increases of the lamellar period. However, PVDF would not be able to incorporate into the wetting PMMA layer directly contacted with the substrate due to the strong affinity of PMMA to the native oxide layer of silicon wafers. Thus, the wetting PMMA layer would be pure PMMA without PVDF, although it can be also possible that PVDF chains could segregate laterally in the first PMMA layer. The result that PVDF chains were localized in the middle of the PMMA lamellae instead of uniform mixing with PMMA blocks, which will be discussed later, could be a supportive evidence for low possibility of PVDF chains in the PMMA lamella at the substrate interface. This situation was also considered when the lamellar period of thin film blends was deduced from the quantized film thickness. However, we were not able to evaluate dependences of the

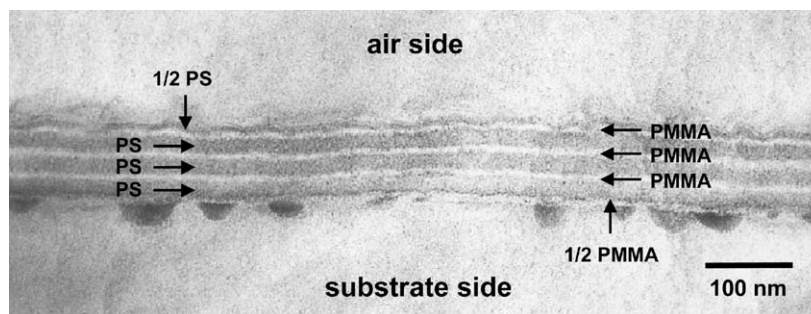


Fig. 2. Cross-sectional TEM image of a PS–PMMA thin film.

degree of swelling on the proximity of the domain to the substrate because of poor developments of steps at the edge of the thin film blends [24,25].

To find whether PVDF chains were uniformly mixed with PMMA chains or localized in the center of PMMA domains, the general behavior in blends of diblock copolymers and homopolymers will be briefly discussed first. In a blend of symmetric A–B diblock copolymers with A homopolymers, A homopolymers can be dissolved in the A lamellar domains. When A homopolymers have a higher molecular weight than the A block, they are confined in the center of the A lamellar domain, corresponding to the so-called ‘dry-brush’ case, instead of uniform mixing due to the entropic origin. The lamellar period (L) in this case can be expressed by

$$L = \frac{L_0}{(1 - \phi)} \quad (1)$$

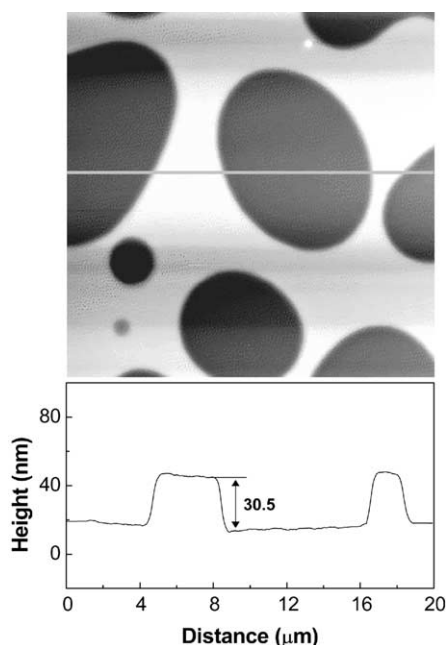


Fig. 3. AFM image of the surface of a thin film blend of PS–PMMA and PVDF with holes in a step height of L . Holes on the film appear as dark areas. The volume fraction of PVDF in the film was 0.13. Along the line in the image, height profile is given below the image.

where L_0 is the lamellar period of pure diblock copolymers and ϕ is the volume fraction of homopolymers in the entire film [24,25]. Contrarily, when A homopolymers have a lower molecular weight than the A block, they are uniformly dissolved in the A lamellar domain of symmetric A–B diblock copolymers, corresponding to the so-called ‘wet-brush’ condition. The dependence of the lamellar period on the volume fraction of homopolymers in uniform distribution is

$$\frac{L}{L_0} = \frac{g(\phi_f, \phi)^{-1/3}}{(1 - \phi)} \quad (2)$$

$$g(\phi_f, \phi) = \frac{[\phi_f + (1 - \phi_f)\phi^2]}{\phi_f(1 - \phi)^2}$$

where ϕ_f is the volume fraction of the block where homopolymers are dissolved [24,25]. The value of ϕ_f is 1/2 for symmetric diblock copolymers. In the case of uniform distribution, intermingling of homopolymer chains with chains of the A block resulted in the increase of the A lamellar thickness. However, by lateral swelling of the A lamellae, the B lamellae should be shrank to maintain uniform density throughout the film. Since the thickness increase of the A lamellae was generally greater than the thickness decrease of B lamellae, the lamellar period was increased by blending of homopolymers. Thus, an increase of the lamellar period by uniformly distributed

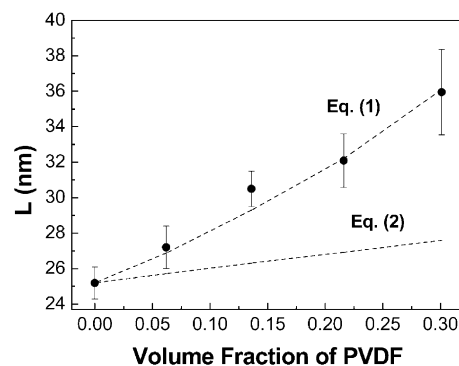


Fig. 4. Lamellar period of a thin film blend of PS–PMMA and PVDF as a function of the volume fraction of PVDF. Curves calculated by Eqs. (1) and (2) are also plotted.

homopolymers is smaller than that by localized homopolymers, as predicted by Eqs. (1) and (2).

In Fig. 4, both lines calculated by Eqs. (1) and (2) are included. As we can see, dependence of the lamellar period on the volume fraction of PVDF exactly followed the predicted line for localization of homopolymers in the middle of lamellar domains. From this result, we found that PVDF chains were localized in the center of the PMMA domains. Because of a negative sign of the Flory–Huggins interaction parameter between PVDF and PMMA [23], uniform distribution of PVDF chains in PMMA domains via intermingling between chains can be expected if the molecular weight of PVDF is sufficiently low to have a benefit in translational entropy by uniform mixing. However, although the molecular weight of PVDF was lower than that of the PMMA block, the PVDF chains could be long enough to require appreciable stretching of the PMMA chains to accommodate the PVDF chains for uniform addition in the PMMA domains, which could cause a substantial decrease in the conformational entropy of the PMMA chains. Thus, localization of PVDF chains in the middle of the PMMA domains could be favored over uniform mixing between PVDF and PMMA chains.

Since the crystallization of PVDF in thin film blends was avoided by quenching, PVDF in the center of amorphous PMMA domains should be in amorphous state. To induce the crystallization of PVDF in thin film blends, the films were annealed again near the crystallization temperature of PVDF. Fig. 5 shows an AFM image of the surface after the crystallization of PVDF when the volume fraction of PVDF in the film was 0.13. As like the surface before the

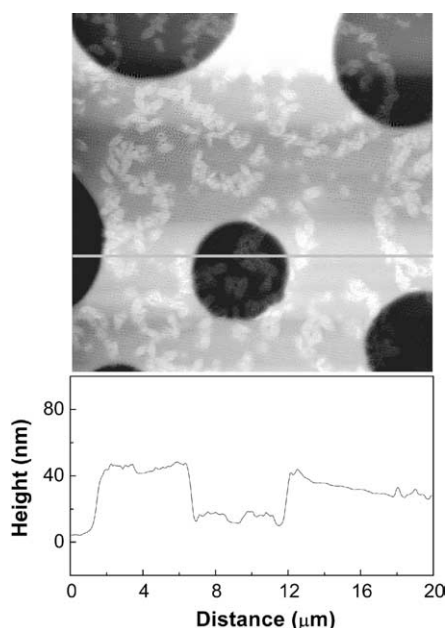


Fig. 5. AFM image of the surface of a thin film blend of PS–PMMA and PVDF after crystallization of PVDF. The volume fraction of PVDF in the film was 0.13. Along the line in the image, height profile is given below the image.

crystallization shown in Fig. 3, holes were maintained, implying that parallel lamellae would not be altered. However, aggregates of ellipsoidal PVDF crystallites, which could be semicrystallites, (ca. $0.90\ \mu\text{m}$ in long axis and ca. $0.44\ \mu\text{m}$ in short axis) were visible all over the surface of the film. On the surface of all thin film blends that we studied with various volume fractions of PVDF, similar crystallites of PVDF were observed. The crystallization of PVDF in thin film blends was performed at the temperature lower than the lower critical solution temperature of the blend of PVDF and PMMA. Thus, phase separation of PVDF and PMMA would not be expected in the bulk blends if the crystallization were performed under the same condition. In the thin film blends, however, amorphous PVDF chains were already localized in the middle of the PMMA lamellae, instead of being uniformly mixed with PMMA chains, before the crystallization of PVDF. In addition, the crystallization was carried out at the temperature above the glass transition temperatures of PMMA and PS. Thus, through mobile PMMA and PS chains, PVDF chains having a low surface energy could migrate to the surface and form small crystallites during the annealing process for the crystallization of PVDF. If all of PVDF chains in the PMMA lamellae move to the surface of the film, the film thickness and the hole depth would be decreased substantially after the crystallization of PVDF. However, although we were not able to quantify changes of the film thickness and the hole depth due to the irregularity of the surface by PVDF crystallites, the decrease would not be large as shown in Fig. 5. Therefore, some of PVDF chains could remain in the PMMA domains after the crystallization. With the present data, we were not able to find whether they are uniformly mixed with PMMA chains and whether they are crystallized in the PMMA domains.

The crystalline structure of PVDF in thin film blends was characterized by FTIR in ATR mode. To distinguish the peaks directly associated with PVDF crystals from PS–PMMA diblock copolymers, the intensity of the carbonyl peak in a thin film blend after the crystallization of PVDF was adjusted to that in a pure PS–PMMA thin film. As shown in Fig. 6, three peaks at 1192 , 1234 , and $1404\ \text{cm}^{-1}$

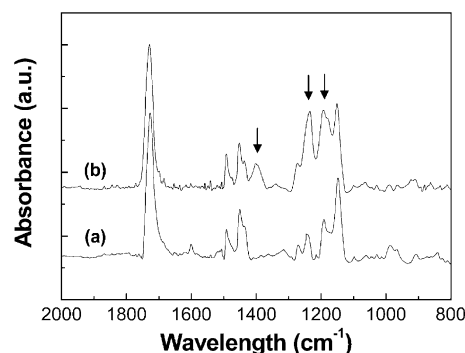


Fig. 6. FTIR spectra: (a) pure PS–PMMA thin film; (b) thin film blend of PS–PMMA and PVDF.

were noticeable in the spectrum of a thin film blend after the crystallization of PVDF, compared to the spectrum of a pure PS–PMMA thin film. PVDF has at least four different crystalline structures, including non-polar α phase and the polar β , γ , and δ phases [23,26]. The peaks at 1192 and 1404 cm^{-1} can be observed in all crystal forms but the peak at 1234 cm^{-1} can be detected only in the γ phase of PVDF [26]. Although the characterization was very limited, PVDF crystallites formed on the surface of thin film blends could be the γ phase. But further studies would be necessary to confirm the crystalline structure and to find causes of such crystalline phase.

4. Conclusions

To demonstrate the strategy of localizing organic functional materials into nanometer-sized domains, we employed a thin film blend of PS–PMMA diblock copolymers with ferroelectric PVDF. Thin films of symmetric PS–PMMA copolymers provided the nanometer-sized PMMA lamellae, macroscopically parallel to the substrate, in which PVDF chains were dissolved due to the miscibility between PVDF and PMMA. Thus, amorphous PVDF chains were effectively confined in the PMMA lamellae of thin film blends. The location of PVDF chains in the PMMA lamellae was investigated by the dependence of the lamellar period on the volume fraction of PVDF, from which we found that PVDF chains were segregated in the middle of the PMMA lamellae. After the crystallization of PVDF, however, some of PVDF migrated to the surface of the film and formed small crystallites. If diblock copolymers were cross-linked, migration of PVDF to the film surface could be reduced so that PVDF crystallites could be confined in nanodomains. We can apply the methodology of blending diblock copolymers with functional polymers in thin films to fabricate organic thin film devices. For example, nanoscale full organic ferroelectric recording media could be effectively produced if ferroelectric PVDF crystallites were incorporated in the cylindrical PMMA nanodomains of PS–PMMA thin film blends, which were perpendicularly oriented to the film plane.

Acknowledgements

This research was supported by National R&D Project for Nano Science and Technology from Korea Institute of Science and Technology Evaluation and Planning (KISTEP).

References

- [1] Hamley IW. The Physics of block copolymers. New York: Oxford University Press; 1998.
- [2] Hamley IW. Nanotechnology 2003;14:R39.
- [3] Park C, Yoon J, Thomas EL. Polymer 2003;44:6725.
- [4] Glass R, Möller M, Spatz JP. Nanotechnology 2003;14:1153.
- [5] Park M, Harrison C, Chaikin PM, Register RA, Adamson DH. Science 1997;276:1401.
- [6] Thurn-Albrecht T, Schotter J, Kästle GA, Emley N, Shibauchi T, Krusin-Elbaum L, et al. Science 2000;290:2126.
- [7] Bronstein L, Antonietti M, Valetsky P. In: Fendler JH, editor. Nanoparticles and nanostructured films. Weinheim: Wiley-VCH; 1998.
- [8] Ng Cheong Chan Y, Schrock RR, Cohen RE. Chem Mater 1992;4:24.
- [9] Saito R, Okamura S, Ishizu K. Polymer 1992;33:1099.
- [10] Moffitt M, McMahon L, Pessel V, Eisenberg A. Chem Mater 1995;7:1185.
- [11] Mayer ABR, Mark JE. Colloid Polym Sci 1997;275:333.
- [12] Fogg DE, Radzilowski LH, Blanski R, Schrock RR, Thomas EL. Macromolecules 1997;30:417.
- [13] Sohn BH, Seo BH. Chem Mater 2001;13:1752.
- [14] Sohn BH, Seo BW, Yoo SI. J Mater Chem 2002;12:1730.
- [15] Coulon G, Russell TP, Deline VR, Green PF. Macromolecules 1989;22:2581.
- [16] Russell TP, Coulon G, Deline VR, Miller DC. Macromolecules 1989;22:4600.
- [17] Foster MD, Sikka M, Singh N, Bates FS, Satija SK, Majkrzak CF. J Chem Phys 1992;96:8605.
- [18] Krausch G. Mater Sci Eng 1995;R14:1.
- [19] Fasolka MJ, Mayes AM. Ann Rev Mater Res 2001;31:323.
- [20] de Jesus MC, Weiss RA, Hahn SF. Macromolecules 1998;31:2230.
- [21] Wang TT, Nishi T. Macromolecules 1977;10:421.
- [22] Tomura H, Saito H, Inoue T. Macromolecules 1992;25:1611.
- [23] Nalwa HS. Ferroelectric polymers. New York: Marcel Dekker; 1995.
- [24] Orso KA, Green PF. Macromolecules 1999;32:1087.
- [25] Smith MD, Green PF, Saunders R. Macromolecules 1999;32:8392.
- [26] Benz M, Euler WB, Gregory OJ. Macromolecules 2002;35:2682.